J Solid State Electrochem (2008) 12:663–669
DOI 10.1007/s10008-007-0399-9

ORIGINAL PAPER

Synthesis and electrochemical characterization of carbon nanotubes decorated with nickel nanoparticles for use as an electrochemical capacitor

Chien-Te Hsieh · Yun-Wen Chou · Wei-Yu Chen

Received: 11 June 2007 / Revised: 5 July 2007 / Accepted: 29 July 2007 / Published online: 25 August 2007

Abstract Attachment of nickel nanoparticles on multi-walled carbon nanotubes (MWCNTs) was conducted to explore the influence of Ni loading on the electrochemical capacitance of MWCNT electrodes. A chemical impregnation leaded to homogeneously disperse Ni particles onto the surface of MWCNTs, and the Ni particles were found to be an average size of 30–50 nm. The capacitive behavior of the MWCNT electrodes was investigated in 6 M KOH, by using cyclic voltammetry (CV), charge–discharge cycling, and ac electrochemical impedance spectroscopy. CV measurements showed that the Faradaic current was found to increase with the Ni coverage, indicating that the presence of Ni would enhance the pseudocapacitance through the redox process. Equivalent circuit analysis indicated that both of electrical connection and charge transfer resistances accounted for the major proportion of the overall resistance and were found to decrease with the amount of nickel. A linearity relationship between the total capacitance and the Ni population reflected that each Ni particle exhibits an identical electrochemical activity in enhancing the electrochemical capacitance. The overall electrochemical capacitance (including double layer capacitance and pseudocapacitance) of Ni-MWCNT electrode can reach a maximum of 210 F/g over 500 cycles.

C.-T. Hsieh (✉) · Y.-W. Chou · W.-Y. Chen
Department of Chemical Engineering and Materials Science,
Yuan Ze University,
Taoyuan 320, Taiwan
e-mail: cthsieh@saturn.yzu.edu.tw

C.-T. Hsieh
Yuan Ze Fuel Cell Center, Yuan Ze University,
Taoyuan 320, Taiwan

Keywords Carbon nanotubes · Electric double-layer capacitance · Nickel nanoparticle · Pseudocapacitance · ac electrochemical impedance

Introduction

Because of their high energy storage capability, electrochemical capacitors (ECs), which still retain the higher power density feature of conventional capacitors, have received a great deal of attention for serving as peak-power energy sources [1–7]. Typically, the energy storage of ECs is either capacitive or pseudo-capacitive in nature [8–11]. The capacitive-type EC is based on charge separation at the electrode material/solution interface, whereas the pseudo-capacitive process consists of Faradaic redox reactions, which occur within the active materials, such as carbon, conducting polymer, metal oxides, and so on.

Porous carbon is the electrode material used most frequently for ECs. Use of highly porous carbon electrodes leads to reaching a large specific capacitance, mainly due to the formation of double layer at electrode surface. Recently, numerous researchers have paid attention on applying multiwalled carbon nanotubes (MWCNTs) as electrode materials [8–17]. They have demonstrated that the MWCNTs and composites composed of MWCNTs and electroactive materials (e.g., conducting polymer and metal oxide) are shown to exhibit the promising applicability to ECs. However, the specific capacitance of MWCNTs is relatively low because of their relatively low surface areas [14]. Therefore, it is more desirable to employ the other contribution from metal catalyst attached on MWCNTs that would provide more sites for reversible redox reactions, thus, giving rise to pseudocapacitance.

It has been reported that nickel and its oxide have been shown to possess an excellent electrochemical activity in alkali electrolyte [2, 18–22]. However, the roles that the attachment of nickel on MWCNTs plays in the enhancement of capacitances have not yet been clearly elucidated. If the active species are deposited over MWCNT electrodes, the attachment of Ni may provide redox activity to enhance the pseudocapacitance. In the present work, a surface modification was employed to prepare well dispersion of Ni nanoparticles onto MWCNTs. Electrochemical characteristics of the resulting capacitors, equipped with as-synthesized Ni-MWCNT composites, are examined by using cyclic voltammetry (CV), charge/discharge cycling, and ac impedance spectroscopy. Also, we proposed an equivalent circuit to the electrochemical impedance behavior of the Ni-MWCNT capacitors.

Experimental section

Preparation and characterization of electrode materials MWCNTs used were prepared via catalytic decomposition of ethylene over Ni catalysts. At first, the MWCNT samples were mixed with 0.1 N nitric acid at 90 °C for a period of 8 h. After that, the acid treated-MWCNT samples were rinsed by D.I. water, until the pH value of the slurry higher than 5. The acid-treated MWCNT samples were then mixed with various concentrations of Ni ionic nitrate (0.1, 0.2, and 0.5 M), and then stirred under Ar atmosphere at 30 °C for 6 h. This wet-impregnation process enables Ni^{2+} ions to interact with MWCNT surface. After that, the ionic-adsorbed MWCNTs were separated from the Ni-salt solution by using a filtration apparatus. Finally, a thermal reduction was performed at 350 °C under a 5 vol.% H_2 atmosphere, thus, giving MWCNTs decorated with Ni nanoparticles. The as-grown MWCNTs were characterized by transmission electron microscope (TEM) (Hitachi H-7500) and X-ray diffraction (XRD) with Cu-Ká radiation using an automated X-ray diffractometer (Shimazu Labx XRD-6000). Specific surface areas and pore volumes of the derived MWCNTs were determined by gas adsorption. An automated adsorption apparatus (Micromeritics, ASAP 2000) was employed for these porous measurements.

Electrode preparation and electrochemical characterization Before the formation of electrodes for electrochemical tests, Ni-MWCNTs were added into a solution of polyvinylidenefluoride (PVdF) in *N*-methyl pyrrolidinone (NMP), and the mixture was mixed at ambient temperature to form carbon slurries. Electrodes were prepared by pressing the slurry on stainless steel foils with a doctor blade, followed by evaporating the solvent, NMP, with a blower dryer. The carbon layer, which consisted of 10 wt% PVdF as binder, was adjusted to have a thickness of 150 μm. This recipe is suitable for preparing the uniform MWCNT electrode with a coating thickness of ca 90–100 μm.

Electrochemical measurements were carried out at ambient temperature using 6 M KOH as the electrolyte solution. A Pt wire was used as the counter electrode and a saturated calomel electrode (SCE) as the reference. The working electrodes were constructed by coating the Ni-MWCNTs onto stainless steel foil (as current collector). Epoxy resin was employed to seal the electrode, allowing an area ca 2×1 cm^2 to be exposed to the electrolyte solution. This sealed method can ensure to prevent unwanted reactions from the backing plate (current collector) in aqueous electrolyte. CV measurements of the MWCNT electrodes were made in the potential range of 0.2 to 1.2 V vs SCE at a scan rate of 30 mV/s. Two electrode cells were used to examine the charge/discharge cycling of the Ni-coated MWCNTs at constant current density. The cells were constructed with two facing carbon electrodes, sandwiching a piece of filter paper as separator. An ac impedance spectrum analyzer (CH Instrument, CHI 608) combined with computer software was employed to measure and analyze the ac impedance behavior of the electrodes. In this work, the potential amplitude of ac was equal to 5 mV, and the frequency was from 100 kHz to 0.1 Hz at open circuit potential (OCP). All electrochemical measurements were performed at ambient temperature.

Results and discussion

A bright-field TEM of nickel particles attached with a high magnification is shown in Fig. 1. This observation reveals that after the deposition of Ni, a number of nanoparticles homogeneously attached on the external surface of MWCNTs. The size of Ni particles varies from 30 to 50 nm. Most particles are quasi-spherical in shape and seem to tightly disperse on the surface of MWCNTs. This proves that our preparation method is able to make the attached metal particles uniformly deposited onto MWCNTs. N_2 adsorption/desorption measurements indicate that all CNT samples are mainly mesoporous, and their specific surface areas range from 105 to 125 m^2/g, according to Brunauer–Emmett–Teller (BET) equation. The influence of the physical structure of the pore of MWCNTs on the performance of capacitors seems to be minor, and thus can be eliminated in this study.

XRD patterns for all Ni-MWCNT products are collected and shown in Fig. 2. We find that similar patterns are obtained for Ni-attached MWCNTs. The peak at ca $2\theta=26°$ corresponds to the graphitic structure of MWCNTs. The XRD shows that Ni nanoparticles are face-center-cubic crystalline, as indicated by the characteristic peaks in Fig. 2.

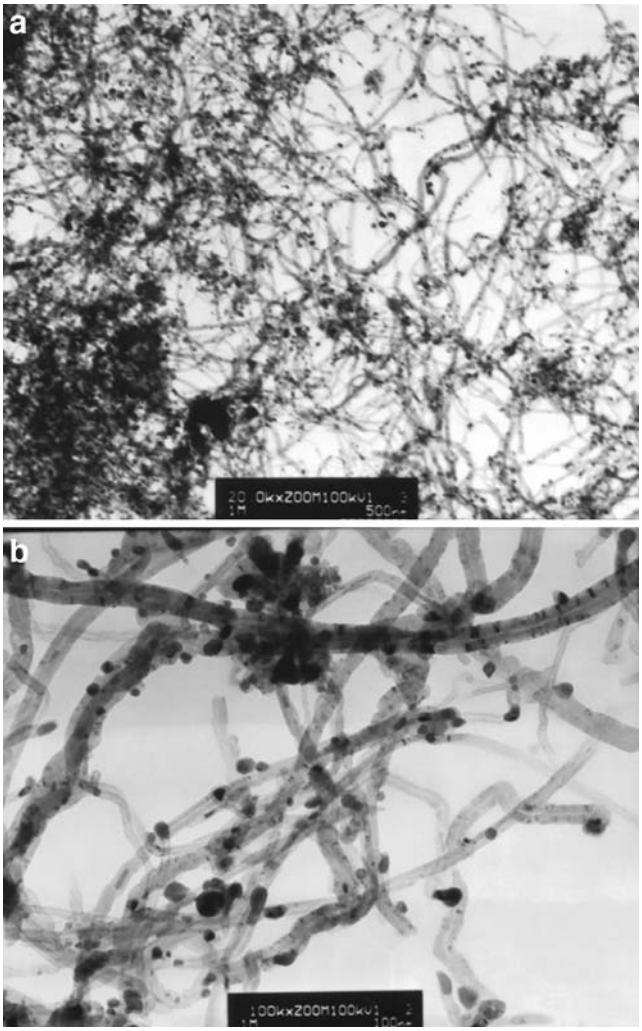

Fig. 1 TEM images at different magnifications: **a** ×20 k and **b** ×100 k, for Ni particles deposited on MWCNTs

As expected, all intensities for Ni crystalline are found to increase with the Ni loading.

The voltammograms generally stabilized after the first cycling, and all the CV plots in the present work are the second-cycle data. Figure 3 shows the CVs for fresh and MWCNT electrodes attached with different Ni molar loadings, i.e., Ni/(C + Ni)=5, 10, and 14 mol%. According to the above calculations, the Ni-MWCNT composites were designated as Ni-CNT5, Ni-CNT10, and Ni-CNT14, respectively. In comparison, the fresh MWCNT electrode exhibits a typical mirror image type of voltammogram within a potential range of 0.2 to 1.2 V vs SCE. Capacitance without Ni attachment on MWCNTs shows a rectangular shape, indicating dominance of double-layer mechanism. In an ideal formation of electric double layer with bases serving as the electrolyte, the equilibrium reaction at MWCNT electrode is due to a simple physical adsorption, by electrostatic forces between the carbon surface and the hydroxyl ions. Basically, the numbers of ions involved in building the double layer match the charge density developed on the MWCNT electrode.

Above the double-layer background current, obvious redox peaks can be observed for all Ni-MWCNT electrodes. At first, the oxidation of metallic nickel in aqueous solution is thought to be [23]

$$Ni + H_2O \leftrightarrow NiO + 2\,H^+ + 2e^- \quad (1)$$

After that, this increase of the current due to the presence of Ni metal can be ascribed to the contribution from the redox reaction in alkali electrolyte

$$NiO + OH^- \leftrightarrow NiOOH + H_2O + e^- \quad (2)$$

The redox reaction of NiO shown in Eq. 2 generally shows a capacitive behavior in its cyclic voltammogram [22], rather than redox peak currents that are generally used for energy storage in batteries. It is believed that nickel oxide in contact with an alkali solution tends to change to nickel hydroxide at particle surface. The nickel hydroxide is expected to form on the surface of nickel oxide, probably within several angstroms [21]. Consequently, the proportion of nickel hydroxide formation would be much more prominent in the case of Ni-MWCNT electrode, thus, resulting in the appearance of anodic and cathodic peaks corresponding to the $Ni(OH)_2$/NiCOOH redox reaction [18, 21, 22], i.e.,

$$Ni(OH)_2 + OH^- \leftrightarrow NiOOH + H_2O + e^- \quad (3)$$

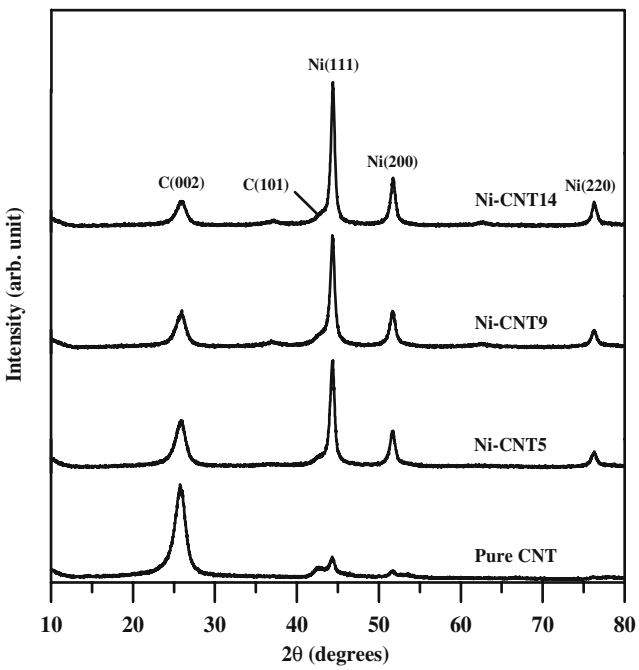

Fig. 2 X-ray diffraction pattern of fresh and Ni-coated MWCNTs showing characteristics crystalline faces of Ni. The peak of C was identified as graphite from the MWCNTs

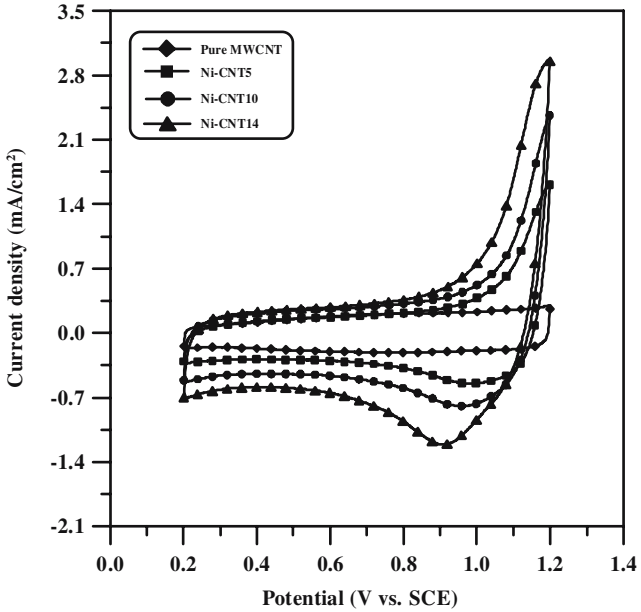

Fig. 3 Cyclic voltammograms of the MWCNT electrodes in 6 M KOH at a scan rate of 30 mV/s

Accordingly, the mechanism in arising the enhancement of capacitance of Ni-MWCNT electrodes discloses two key factors: (1) Ni nanoparticles act as reversible redox sites; (2) MWCNTs not only play a support for deposition of Ni particles but also an electric conductor for electron transport. As it behaves as an excellent conducting property, the MWCNT would show exceptional competence for the above undertaking. As shown in Fig. 4, this peak current density is found to increase with the Ni loading onto MWCNTs. This linearity relationship reflects that the Ni density increases proportionally with the charge transfer, i.e., pseudocapacitance. This finding reveals that each Ni particle has an identical electrochemical activity even at high Ni loading.

In addition, it is noticed that the voltammogram at high sweep rate of 30 mV/s, in which current quickly reaches a truly horizontal value after reversal of the potential sweep, is observed for fresh MWCNT electrode. However, these CV plots for all Ni-MWCNT electrodes have a slight delay in potential reversal. Basically, as for the porous carbon electrodes, the presence of narrow pore probably retards the motion of electrolytes and thus increases the ohmic resistance of electrolytes along the axial direction of micropores, which would combine with the existence of the distributed capacitance to cause the delay of current inversion [24]. This phenomenon is presumably due to the ionic diffusion resistance, contributed from the pore blockage by Ni particles.

To illustrate the influence of Ni attachment on the performance of constant-current charge and discharge, Fig. 5 shows the potential against time curves of all Ni-MWCNT capacitors charged and discharged at a constant current of 0.5 mA/cm^2. In comparison, the Ni-CNT14 capacitor appears the highest discharge capacitance. Based on the results of charge/discharge cycling, the specific discharge capacitance of a single electrode in the capacitors can be calculated according to [25, 26]

$$C = \frac{2It}{W\Delta E} \tag{4}$$

where I is the discharge current, t the discharge time, W the carbon fabric mass on an electrode, and ΔE the potential difference in discharge, excluding the portion of IR drop. The factor of 2 comes from the fact that the total capacitance measured from the test cells is the sum of two equivalent single-electrode capacitors in series. The capacitances of different electrodes obtained at the same discharge currents have the following order: Ni-CNT14 (240 F/g)>Ni-CNT10 (185 F/g)>Ni-CNT5 (135 F/g)>pure MWCNT (88 F/g). As expected, the specific capacitance was found to increase with the loading of nickel, which is in agreement with the results from cyclic voltammetric measurements. Comparing with the capacitances of pure MWCNT and Ni-CNT14 capacitors, there is ca 173% capacitance increase achieved through introduction of Ni nanoparticles (e.g., an increase from 88 to 240 F/g at a current of 1 mA, or a current density of 0.5 mA/cm^2).

The stability of the prepared capacitors can be examined by conducting repeated charge/discharge cycling. Two capacitors equipped with pure MWCNT and CNT-Ni14 electrodes were charged and discharged at 0.5 mA/cm^2 to confirm the

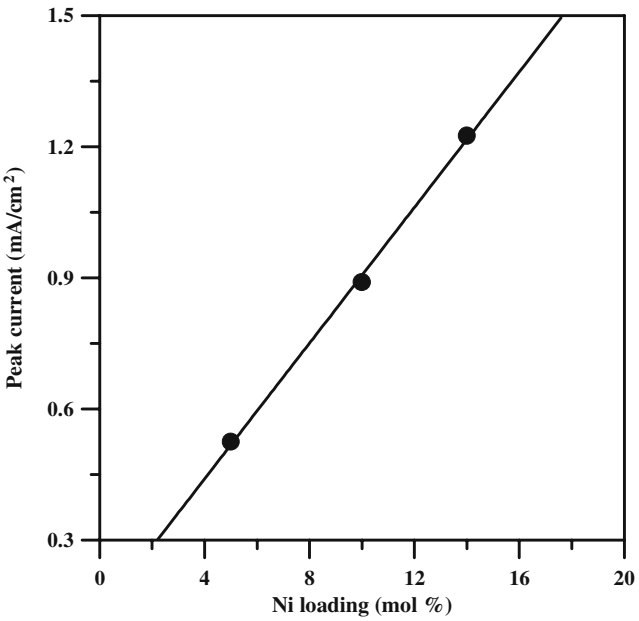

Fig. 4 Variation of peak current at 0.9 V vs SCE with Ni loading for different MWCNT electrodes

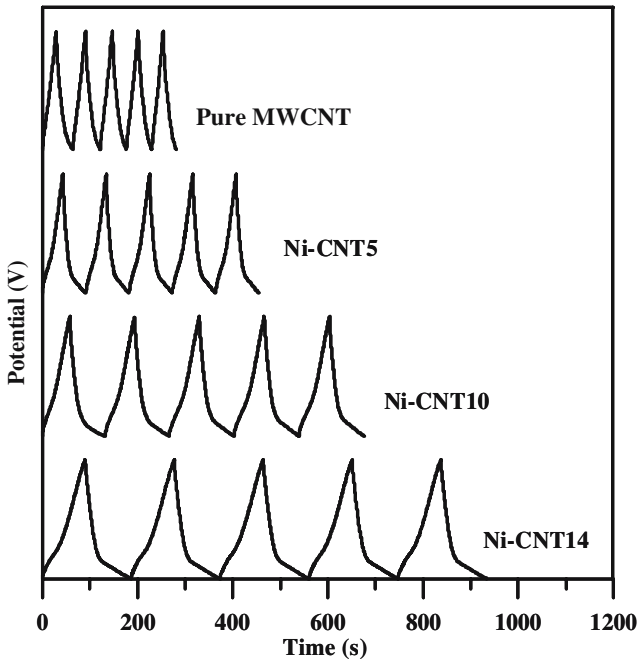

Fig. 5 Comparison of charge–discharge curves of pure MWCNT and Ni-MWCNT electrodes at 0.5 mA/cm^2 in 6 M KOH

stability. The coulombic efficiency (η) of an electrochemical capacitor can be calculated from the equation [27]

$$\eta(\%) = \frac{t_D}{t_C} \times 100 \tag{5}$$

where t_D and t_C are the times required for discharge and charge, respectively. The variation of coulombic efficiency with cycle number keeps a high value of 99.5% for both of capacitors. As shown in Fig. 6, the Ni-CNT14 capacitor has stable capacitance (about 210 F/g) over 500 cycles. There is only 12.5% capacitance loss during cycling in the capacitors, equipped with Ni-MWCNT composites.

The technique of ac impedance spectroscopy was further employed to analyze the electrochemical behavior of Ni-MWCNT electrodes. The impedance spectra of different MWCNT electrodes are shown as Nyquist plots in Fig. 7a. The OCP was found to be ca 0.7 V vs SCE for all electrodes. An intersecting occurs in the real axis in the high frequency region, followed by a single quasi-semicircle in low frequency region. This semicircle in the high-frequency region can be attributed to (1) the presence of an interface, between the MWCNTs and the current collector, and (2) the presence of a RC loop involving a double-layer capacitance in parallel with a resistance [1, 5]. Then, the plot transforms to an almost vertical line with decreasing frequency. The almost vertical lines (ca 70–75° all CNT electrodes) at low frequencies correspond to the capacitive response of the porous carbons [1, 4]. The non-vertical slope of the impedance plot at low frequency of electrochemical capacitor may be ascribed to (1) different pore-size-distribution carbons, and (2) low mobility of ions inside the electrodes, or (3) the combination of both [28 30].

To describe the influence of Ni loading on the electrochemical behavior, an equivalent circuit for Ni-MWCNT electrodes should involve the following circuit elements [26]: the bulk solution resistance, R_s; the double layer capacitance, C_{dl}; the Faradaic resistance, R_F, corresponding to the reciprocal of the potential-dependent charge transfer rate in reactions like Eqs. 1–3; a pseudocapacitance, C_p, associated with the potential dependence of redox-site concentration in Eqs. 1–3; and C_b and R_b due to the impedance between the MWCNT and the backing plate for the electrical connection. The combination of the circuit elements is proposed and shown in Fig. 7b. Accordingly, the overall impedance, Z, of the equivalent circuit is given by

$$Z = R_s + \frac{R_b}{j\omega R_b C_b + 1} + \frac{1}{j\omega C_{dl} + \frac{j\omega C_p}{j\omega R_F C_p + 1}} \tag{6}$$

The above equation can be divided into two limiting cases: low- and high-frequency regions. The impedance in low-frequency region suggests the pure capacitive behavior [5], where the overall capacitance, C_{dl} and C_p, of Ni-MWCNT electrode can be estimated. At sufficiently high frequencies, Eq. 6 would correspond to a locus showing the solution, the electrical connection resistance, and the charge transfer resistance, i.e., R_s, R_b, and R_F.

Eq. 6 together with the impedance data in Fig. 7a was employed to estimate the values of the elements of the equivalent circuit in Fig. 7b. Here, Z-view computer software

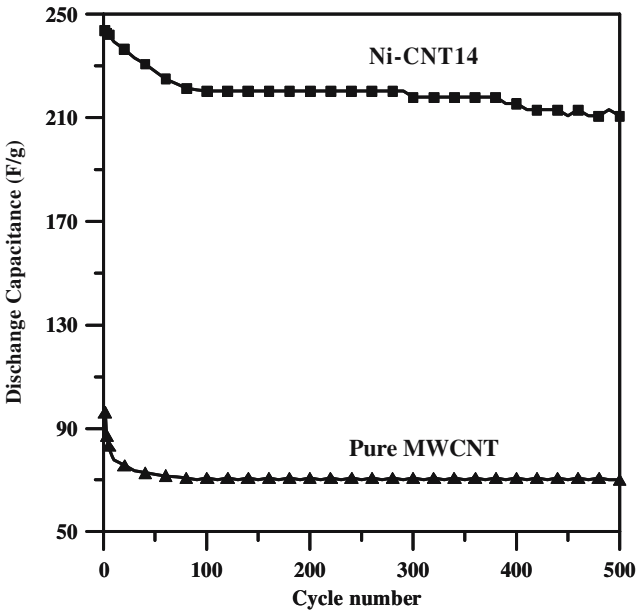

Fig. 6 Variation of capacitance stability with cycle number for MWCNT electrode charged and discharged at 0.5 mA/cm^2 in 6 M KOH

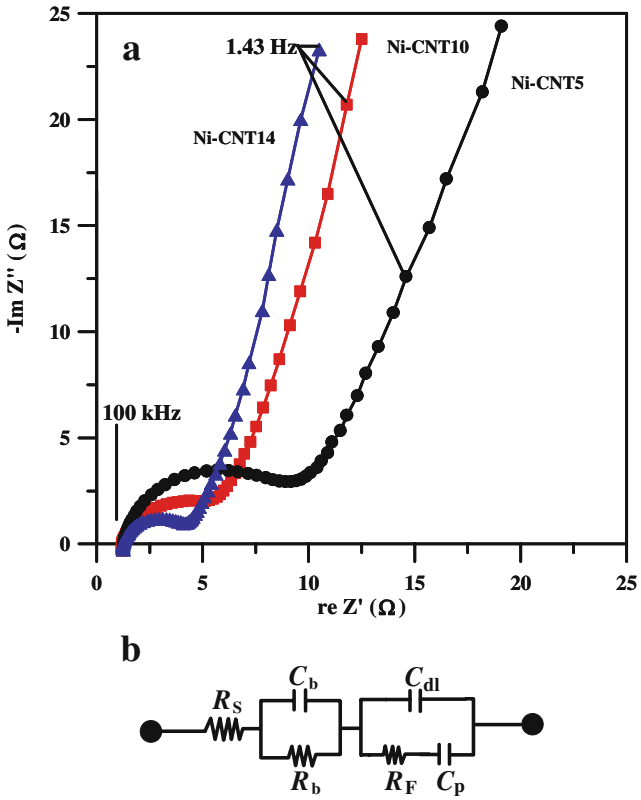

Fig. 7 **a** Nyquist impedance plots of MWCNT electrodes in 6 M KOH with frequency ranging from 100 kHz to 1.43 Hz. **b** Equivalent circuit for the impedance spectra of MWCNT electrodes

was applied here to resolve each components of the circuit within a small error (<10 %). These calculated values are summarized in Table 1. The bulk solution resistance was found to be small and showed little variation with the population of Ni particles. The electrical connection between the MWCNTs and the current collector has been significantly improved due to the introduction of nickel. This can be attributed to a fact that metallic Ni possesses an excellent electric conductivity. The overall capacitance, $C_{dl} + C_p$, obtained from impedance analysis is an increasing function of the Ni coverage, which is analogous to that observed from CV measurement. Here the value of C_b can be negligibly small compared to the overall capacitance. Again, this capacitance enhancement can be ascribed to the existence of metallic Ni onto MWCNTs. After the attachment of Ni,

Table 1 Components of the equivalent circuit fitted for the impedance spectra of Ni-MWCNT electrodes

Electrode	R_s (Ω)	R_c (Ω)	C_c (μF/cm^2)	R_F (Ω)	$C_{dl} + C_p$ (F/g)
Ni-CNT5	1.39	7.07	25.4	13.1	139
Ni-CNT10	1.32	3.58	42.8	9.74	189
Ni-CNT14	1.37	2.63	55.1	5.99	237

the Ni-MWCNT electrode gives the highest capacitance of 237 F/g. Data from Table 1, the overall capacitance was plotted against the Ni loading in Fig. 8. This linear relationship reveals that each Ni particle over MWCNT surface has the same redox activity. From the slope of the linearity plot, the metallic Ni can contribute a specific capacitance as high as 217 F/g, which is almost equal to the energy storage capability of NiO in alkali electrolyte [18].

Here, we notice that both of resistances (i.e., $R_b + R_F$) are found to decrease with the Ni proportion on MWCNTs, as indicated in Table 1. The overall resistance determined is the so-called equivalent series resistance, R_{es} ($=R_s + R_b + R_F$), which is composed of bulk solution resistance, connection resistance, and charge transfer resistance [31]. The R_F value for each Ni-MWCNT electrode could account for a major proportion of the overall resistance, whereas the R_b plays the minor role. It has been emphasized in the proceeding section that the presence of MWCNTs may effectively reduce the resistance of interfacial interface between the electroactive materials and the back plate. This may result in the smaller interfacial resistance. The decrease of charge transfer resistance with Ni loading indicates that the redox rate (Eq. 1) would be enhanced due to the presence of Ni particle. Therefore, the higher metallic Ni surface coverage onto MWCNT would impart not only a better electrical conductivity but also a lower charge transfer resistance. As expected, a decreasing relationship between the equivalent series resistance (R_{es}) and the Ni loading can be observed, as shown in Fig. 8. However, excessive Ni nanoparticles coated on MWCNT surface may cause a continuous nickel layer, possibly reducing the electrochemical redox kinetic. Accord-

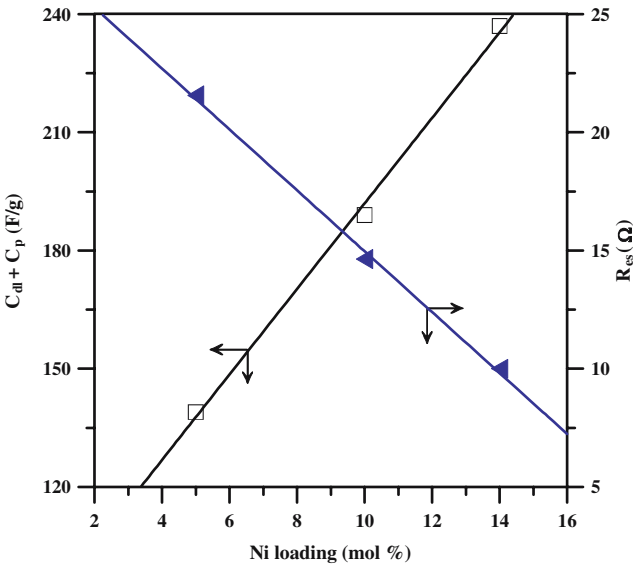

Fig. 8 Variation of overall specific capacitance (C_t) and equivalent serial resistance (R_{es}) with Ni loading onto MWCNTs, determined from the equivalent circuit, as shown in Fig. 7b

ingly, further work is needed to clarify an optimal particle size and the Ni loading amount on the enhancement of capacitance of Ni-MWCNT capacitors.

Conclusions

The present work demonstrated that the attachment of metallic Ni effectively enhances the electrochemical capacitance of MWCNT electrodes in KOH solution. A chemical impregnation leaded to homogeneously disperse Ni particle onto the surface of MWCNTs, which was oxidized by nitric acid treatment. The Ni particles were found to be an average size of 30–50 nm. CV measurements showed that the presence of Ni particle significantly enhances the electrochemical capacitance. The Faradaic current (i.e., peak current) linearly increased with the Ni loading, indicating that the population of Ni coverage promotes the electrochemical redox process. This indicates that attached nickel can be served as a redox site in facilitating an excess specific capacitance, i.e., pseudocapacitance.

Equivalent circuit analysis on the ac impedance results showed that the total resistance of MWCNT electrodes was mainly attributed to the charge transfer and the electrical connection resistances. Both of the two resistances were found to decrease upon the introduction of nickel. This indicated that the Ni attachment would improve not only the conductivity of MWCNT electrodes but also the charge transfer of redox reaction. Through the introduction of Ni nanoparticles, the overall specific capacitance of Ni-MWCNT electrode was found to be a great value of ca 237 F/g. The linearity relationship between the total capacitance and the Ni loading reflected that each Ni particle has an identical electrochemical activity in KOH electrolyte at different Ni densities.

Acknowledgments The authors gratefully acknowledge the financial support from the National Science Council (NSC) and the Ministry of Education (MOE) of Taiwan, Republic of China (R.O.C).

References

1. Conway BE (1999) Electrochemical supercapacitors: Scientific fundamentals and technological applications. Klumer Academic/ Plenum Publishers, New York
2. Xu MW, Bao SJ, Li HL (2007) J Solid State Electrochem 11:372
3. Zhou YK, He BL, Zhang FB, Li HL (2004) J Solid State Electrochem 8:482
4. Kinoshita K (1987) Carbon: Electrochemical and Physicochemical Properties. Wiley, New York
5. Nian JN, Teng H (2005) J Phys Chem B 109:10279
6. Wang YG, Zhang XG (2004) Electrochim Acta 49:1957
7. Shiraishi S, Kurihara H, Shi L, Nakayama T, Oya A (2002) J Electrochem Soc 149:A855
8. Kim JH, Nam KW, Ma SB, Kim KB (2006) Carbon 44:1963
9. Zhang B, Liang J, Xu CL, Ruan BQ, Wu DH (2001) Mater Lett 51:539
10. Chen JH, Li WZ, Wang DZ, Yang SX, Wen JG, Ren ZF (2002) Carbon 40:1193
11. Shiraishi S, Kurihara H, Okabe K, Hulicova D, Oya A (2002) Electrochem Commun 4:593
12. Yang ZH, Wu HQ (2001) Chem Phys Lett 343:235
13. Ahn HJ, Sohn JI, Kim YS, Shim HS, Kim WB, Seong TY (2006) Electrochem Commun 8:513
14. Wu YT, Hu CC (2004) J Electrochem Soc 151:A2060
15. An KH, Kim WS, Park YS, Choi YC, Lee SM, Chung DC, Bae DJ, Lim SC, Lee YH (2001) Adv Mater 13:497
16. An KH, Jeon KK, Heo JK, Lim SC, Bae DJ, Lee YH (2002) J Electrochem Soc 149:A1058
17. Park JH, Ko JM, Park OO (2003) J Electrochem Soc 150:A864
18. Tai YL, Teng H (2004) Carbon 42:2329
19. Liang K, An K, Lee Y (2005) J Mater Sci Technol 21:292
20. Lee JY, Liang K, An KH, Lee YH (2005) Synth Met 150:153
21. Nam KW, Lee ES, Kim JH, Lee YH, Kim KB (2005) J Electrochem Soc 152:A2123
22. Srinivasan V, Weidner, JW (1997) J Electrochem Soc 144:L210
23. Pourbaix M (1974) Atlas of electrochemical equilibria in aqueous solutions. National association of corrosion engineers, Houston
24. de Levie R (1963) Electrochim Acta 8:751
25. Hsieh CT, Teng H (2001) Carbon 40:667
26. Nian YR, Teng H (2002) J Electrochem Soc 149:A1008
27. Osaka T, Liu X, Nojima M, Momma T (1999) J Electrochem Soc 146:1724
28. Song HK, Sung JH, Jung YH, Lee KH, Dao LH, Kim MH, Kim HN (2004) J Electrochem Soc 151:E102
29. Itagaki M, Suzuki S, Shitanda I, Watanabe K, Nakazawa H (2007) J Power Souces 164:415
30. Lee JG, Kim JY, Kim SH (2006) J Power Souces 160:1495
31. Yoon S, Lee J, Hyeon T, Oh SM (2000) J Electrochem Soc 147:2507